Tectonophysics 608 (2013) 545–551

Contents lists available at ScienceDirect

Tectonophysics

journal homepage: www.elsevier.com/locate/tecto

Rheological contrast between serpentine species and implications for slab–mantle wedge decoupling

Ken-ichi Hirauchi *,[1], Ikuo Katayama

Department of Earth and Planetary Systems Science, Graduate School of Science, Hiroshima University, 1-3-1 Kagamiyama, Higashi-Hiroshima, Hiroshima 739-8526, Japan

ARTICLE INFO

Article history:
Received 8 April 2013
Received in revised form 22 July 2013
Accepted 19 August 2013
Available online 27 August 2013

Keywords:
Decoupling
Mantle wedge
Olivine
Serpentine
Subduction zone
Rheological contrast

ABSTRACT

Serpentine is considered the main hydrous mineral to cause significant weakening at the slab–mantle interface; however, despite the possible presence of lizardite/chrysotile (liz/ctl) and antigorite (i.e., low- and high-temperature serpentine species, respectively) at the base of the mantle wedge, the differences in rheological properties between these two serpentine types are poorly understood. To investigate the effect of serpentine speciation on slab–mantle decoupling, we performed a series of two-layer shear deformation experiments on liz/ctl, antigorite, and olivine at $P = 1$ GPa and $T = 250$–300 °C, using a Griggs-type solid-medium apparatus. With increasing shear strain (γ up to ~5), the liz/ctl and antigorite samples evolved to deform predominantly by slip or glide on the (001) basal plane, whereas the olivine sample deformed by a combination of brittle and crystal-plastic mechanisms. The contrasting amount of rotation of strain markers between layers demonstrates that the shear strain of liz/ctl is significantly lower than that of antigorite, possibly arising from differences in interlayer bond strength. The strain contrasts between serpentines and olivine were $\gamma_{liz/ctl}/\gamma_{ol} = 9$–$12$ and $\gamma_{atg}/\gamma_{ol} = 1$–$2$. Our results indicate that assuming a thin, serpentinized layer upon a subducting slab, significant decoupling can occur only where liz/ctl is stable in the layer. Thus, the distribution of serpentine species in the hydrated mantle wedge is a critical factor that controls the degree of decoupling along the slab–wedge interface, at depths below the seismogenic zone.

1. Introduction

Intermediate-depth intraslab earthquakes and arc volcanoes are intimately linked to the release of H_2O-rich fluids by dehydration reactions in the subducting slabs (e.g., Kirby et al., 1996). The thermal structure of subduction zones provides important clues to understanding these geological processes. Analytical and numerical models have shown that a number of important parameters control the thermal structure of a subduction zone (Peacock, 1996, 2003; Syracuse et al., 2010; van Keken, 2003): (1) the slab dip, and age and convergence rate of the subducting slab; (2) the geometry and vigor of flow, the latter of which is strongly controlled by rheology, in the mantle wedge; and (3) the rate of shear heating.

Beneath the arc, subduction of oceanic lithosphere induces corner flow (convection) in the mantle wedge through viscous coupling along the slab–wedge interface (McKenzie, 1969). In the wedge corner, hot mantle material rises from great depths to replace cold material. This upward advection maintains the high temperatures required for partial melting in the mantle wedge (e.g., Tatsumi et al., 1983); however, beneath the forearc, a variety of geophysical data (e.g., Currie and Hyndman, 2006; Furukawa and Uyeda, 1989; Stachnik et al., 2004) suggest that conductive cooling due to the incoming oceanic lithosphere is dominant over advective heat transport by corner flow, keeping the mantle wedge corner relatively cold and stagnant.

To achieve a cold wedge nose, some form of decoupling between the subducting slab and the overlying mantle wedge is necessary. Numerical models have demonstrated that decoupling is required to a depth significantly below the downdip limit of the seismogenic zone (e.g., Abers et al., 2006; Conder, 2005; Furukawa, 1993; Kneller et al., 2005, 2007; Wada et al., 2008), because the presence of decoupling causes significant attenuation of subduction-related plate-driving forces. Previous studies have used a variety of approaches to simulate slab–mantle decoupling. Recently, Wada et al. (2008) used a thin, low-viscosity layer along the slab–wedge interface, and revealed that an increase in the viscosity contrast between the layer and the overlying wedge induced a landward shift in the trenchward limit of convection, leading to widening of the stagnant mantle wedge.

The addition of slab-derived fluids to the forearc mantle wedge might cause the formation of hydrous minerals such as serpentine (lizardite, chrysotile, and antigorite), brucite, and talc (Hyndman and Peacock, 2003). Serpentine minerals [generalized formula $Mg_3Si_2O_5(OH)_4$] are the main hydrous minerals in hydrated ultramafic rocks, because the Mg:Si ratio of serpentine (1.5) lies between that of olivine (2) and orthopyroxene (1). Lizardite and chrysotile are polymorphs stable at temperatures below ~300–400 °C (e.g., Evans, 2004), whereas antigorite

* Corresponding author. Tel.: +81 54 238 4735; fax: +81 54 238 0491.
E-mail address: skhirau@ipc.shizuoka.ac.jp (K. Hirauchi).
[1] Now at the Department of Geosciences, Graduate School of Science, Shizuoka University, 836 Ohya, Suruga-ku, Shizuoka 422-8529, Japan.

0040-1951/$ – see front matter © 2013 Elsevier B.V. All rights reserved.
http://dx.doi.org/10.1016/j.tecto.2013.08.027

is stable over a wide range of *P*–*T* conditions (up to $T = 600$ °C at $P = 4$ GPa) (e.g., Bromiley and Pawley, 2003; Komabayashi et al., 2005; Ulmer and Trommsdorff, 1995). On the basis of calculated *P*–*T* paths of slab surfaces in oceanic and continental subduction zones (e.g., Peacock, 2003; Syracuse et al., 2010; Wada and Wang, 2009), we suggest that all serpentine phases are stable at the base of the mantle wedge corner, depending on the thermal structure of the incoming lithosphere (primarily a function of slab age).

Recent high-pressure (>1 GPa) deformation experiments showed that serpentine undergoes crystal-plastic or semi-brittle deformation (Amiguet et al., 2012; Chernak and Hirth, 2010; Hilairet et al., 2007; Hirauchi et al., 2010a; Katayama et al., 2009). Extrapolation of the flow law derived for antigorite by Hilairet et al. (2007) to geological conditions predicts viscosities that are substantially lower than those of olivine; however, the differences in rheological properties between low- and high-temperature serpentine species are still poorly constrained. In the present study, we performed two-layer shear deformation experiments under *P*–*T* conditions corresponding to the mantle wedge corner. The effect of serpentine species on slab–mantle decoupling was evaluated in terms of the style of mantle wedge flow.

2. Experimental and analytical procedures

2.1. Starting materials

The starting materials for low-*T* and high-*T* serpentines are natural serpentinites collected from the Mineoka ophiolite, central Japan, and from the Nagasaki metamorphic rocks, southwest Japan, respectively (Fig. 1A, B). Low-*T* serpentines exhibit mesh textures and bastite pseudomorphs after olivine and orthopyroxene (Wicks and Whittaker, 1977): the former consists of polyhedral, isotropic "cores" (a mixture of chrysotile nanotubes and magnetite dust) enclosed by fibrous "rims" (stacks of lizardite crystals) (Fig. 1A), whereas the latter retains relict cleavage in the form of serpentine (lizardite) platelets (Hirauchi et al., 2010a). High-*T* serpentines show interpenetrating or interlocking textures (Fig. 1B) (Wicks and Whittaker, 1977) that consist of near-randomly oriented, platy or acicular antigorite grains, ranging from 10 to 150 μm in length, with finely disseminated magnetite (Fig. 1B). The starting materials for olivine are hot-pressed aggregates prepared from a sample of San Carlos olivine (Fo_{90}). Olivine grains (10–20 μm in size) are equant and polygonal with near-random orientations (Fig. 1C). Olivine aggregates also contain intra- and inter-granular fluid inclusions (Fig. 1D), indicating that they formed under water-saturated conditions.

2.2. Deformation experiments

Shear deformation experiments were conducted using a modified Griggs-type solid-medium apparatus installed at Hiroshima University, Japan, at $P = 1.0$ GPa, $T = 250$ and 300 °C, and at constant shear strain rates ranging from 2.4×10^{-5} to 6.3×10^{-4} s^{-1} (Table 1; Fig. 2) [see Ando et al. (2006) for details of the experimental apparatus]. For the experiments, specimens were cored to make a right cylinder with a diameter of 4.0 mm, and then both ends of the cylinder were cut at an angle of 45° to the long axis, to form slices with a thickness of ~400 μm. Each sample was cut into two halves normal to the plane and separated by a thin film of Ni (20 μm thickness). The two sets of samples were sandwiched between alumina pistons in a simple shear geometry, as shown in Fig. 2. The piston–sample assembly was surrounded by a Ni capsule, and the oxygen fugacity was buffered by Ni/NiO equilibrium. We made tiny grooves at the interface between the sample and piston to prevent slips during deformation.

Pressure was first raised to 400 MPa, then temperature was increased at a rate of ~20 °C/min. The pressure was then raised again to the desired value of 1.0 GPa. Temperature was monitored by two Pt/Rh thermocouples placed close to the center of the Ni capsule. The temperature difference between the two thermocouples was usually within ~5–10 °C. After the temperature had stabilized, the piston was advanced at a constant rate using a servo-motor until the desired strain was attained. Experiments were quenched rapidly by switching off the thermo-controller and then pressure was reduced.

Shear strain (γ) was assessed from the rotation of Ni strain markers in recovered samples (Fig. 3). Strain markers were initially oriented perpendicular to the shear direction. Compressional strain, which for most samples was about an order of magnitude smaller than the shear strain, was measured from the change in specimen thickness after deformation.

Major-element analyses of serpentine minerals were performed using an electron probe microanalyzer (EPMA; JEOL JXA-8200) housed at the Natural Science Center for Basic Research and Development (N-BARD), Hiroshima University, Japan, with a 15 kV accelerating

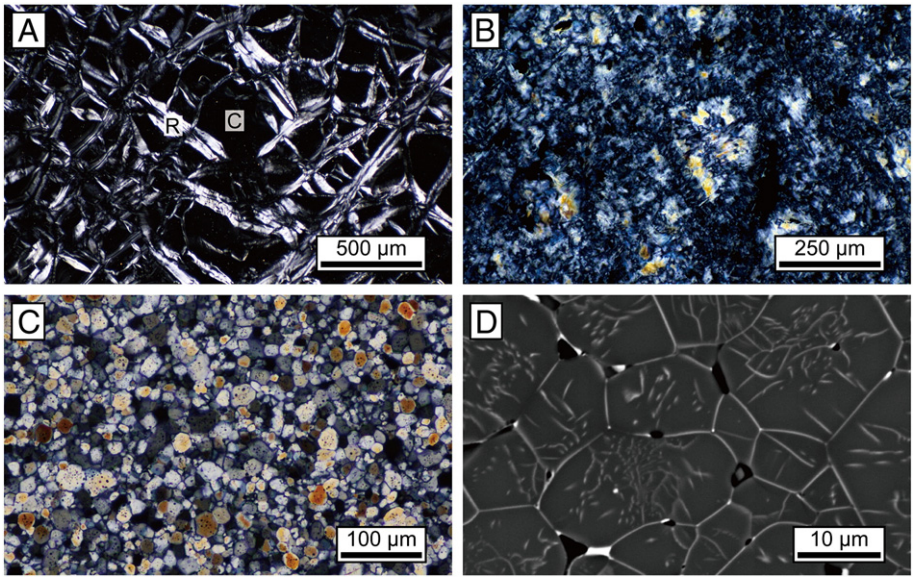

Fig. 1. (A–C) Optical photomicrographs of starting materials in cross-polarized light. (A) Liz/ctl sample, exhibiting mesh texture with serpentine after olivine. Polyhedral, isotropic cores "C" are surrounded by fibrous rims "R". (B) Antigorite sample with interlocking texture. Randomly oriented antigorite blades with finely disseminated magnetite. (C) Olivine sample, with equant and polygonal grains and near-random orientations. (D) Back-scattered electron image of the starting material (olivine sample) decorated by oxidation in air at $T = 900$ °C for ~3 h. Grains contain intra- and inter-granular fluid inclusions. Dislocations are bright dots or lines. Note that the dislocation density of olivine crystals is 1.4×10^{12} m^{-2}.